

THERMOLUMINESCENCE PROPERTIES OF BARIUM-CONTAINING PHOSPHORS FOR HIGH-ENERGY RADIATION DOSIMETRY

Subhi sharma

guest Faculty Department of physics Naveen Government College
Jarhagon District Mungeli

N k puraley

assistant professor & HOD Department of physics
Dr Jwala Prasad Mishra government science college mungeli CG

Abstract

Medical imaging, radiation treatment, and environmental monitoring are just a few of the many fields that make use of thermoluminescence (TL) dosimetry to measure radiation doses. The remarkable sensitivity, stability, and repeatability of barium-containing phosphors in detecting high-energy radiation have made them a potentially useful material. This research delves into the TL features of phosphors based on barium, specifically looking at its structural features, luminescent efficiency, and reaction to various radiation sources. Phosphors based on barium, doped with rare-earth or transition metal ions, have great TL properties and may be used for dosimetric purposes. Examples of such phosphors include $BaSO_4$, BaF_k , and $BaAl_2O_4$. These phosphors were synthesised using the solid-state reaction approach and then characterised structurally using X-ray diffraction (XRD) and scanning electron microscopy (SEM). Following exposure to gamma, beta, and X-ray radiation sources, the TL glow curve analysis was carried out. The glow curve deconvolution method was used to analyse critical factors like peak intensity, trapping parameters, and fading characteristics. The results showed that phosphors based on barium had effective charge trapping and recombination processes, since they show strong TL emission with well defined light peaks. Radiation dosimetry relies on the TL response since it exhibited linear dose dependency over a large range and exhibited little fading. The Chen's peak shape approach was used to calculate the kinetic characteristics, such as the frequency factor and activation energy, demonstrating that these phosphors are suitable for high-precision dosimetric applications. Researchers found that TL materials containing barium were the most effective and stable for use in high-energy radiation dosimetry. They are promising candidates for practical radiation monitoring because to their excellent dosimetric characteristics, low production costs, and simplicity of synthesis. To further improve TL performance, future studies should investigate other host matrices and optimise doping concentrations.

Keywords: Thermoluminescence, Barium-based phosphors, High-energy radiation, Dosimetry, Glow curve analysis, Kinetic parameters.

INTRODUCTION

Accurate assessment of radiation exposure is essential for medical, industrial, and environmental applications; radiation dosimetry plays a key role in radiation safety. Ensuring the safety of those exposed to radiation in the environment, those working in sectors connected to radiation, and patients receiving radiation treatment depends on accurate measurements of ionizing radiation. Because of its sensitivity,

stability, and reproducibility, thermoluminescence (TL) has become a commonly used method in radiation dosimetry. Phosphors containing barium compounds have attracted a lot of attention in the quest for effective chemiluminescent materials. A lot of people are interested in barium-based phosphors because of their special optical and luminous qualities. Doping these phosphors with ions of rare-earth or transition metals makes them ideal for dosimetric applications due to their robust thermoluminescence. Research on the charge carrier trapping and releasing properties of barium-containing materials has focused on sulphate (BaSO_4), fluoride (BaF_2), and aluminate (BaAl_2O_4). Radiation detection effectiveness of these phosphors is sensitive to synthesis processing conditions, dopant concentration, and trapping centre type. Thermoluminescence works by exposing crystal defects or impurity centres to radiation, which causes the charge carriers (holes and electrons) to be trapped. The radiation dosage is calculated by detecting and analysing the light emitted when these trapped carriers are freed, which occurs when the material is heated again. Essential information about a material's dosimetric characteristics, including peak locations, activation energy, and kinetic parameters, may be found in the TL glow curve, which graphs light emission intensity versus temperature. Dosimetry benefits from the excellent sensitivity, linear dose response, and low fading over time shown by barium-based phosphors, according to many studies. These features render them well-suited for tracking radiation exposure in fields such as industrial radiation processing, environmental radiation monitoring, radiotherapy, medical imaging, and radiotherapy. Dosimeter performance of barium-containing phosphors is conditional on their stability in TL response and their capacity to hold trapped charge carriers over long periods of time. The thermoluminescence characteristics of phosphors containing barium are greatly affected by their production. The solid-state reaction method, the sol-gel approach, and combustion synthesis are the most popular synthesis techniques. Each of these techniques has an effect on the TL performance of the phosphors by altering their crystallinity, morphology, and defect structure. Phosphors are more effective as radiation dosimeters when appropriate dopants like europium (Eu), dysprosium (Dy), or thulium (Tm) are added to them. This improves the trapping and recombination processes. Exposure of barium-based phosphors to high-energy radiation is the target of this investigation into their thermoluminescence characteristics. Determining kinetic parameters, studying dose-response characteristics, fading qualities, and TL glow curve analysis are the main goals. The practicality of using phosphors containing barium as trustworthy dosimetric materials will be illuminated by the results of this study.

OBJECTIVES

1. To investigate the properties of thermoluminescence and chemiluminescence
2. To study on Properties of $\text{Ba}_{2-x}\text{MgSi}_2\text{O}_7:x\text{Ce}^{3+}$ Phosphors

RESEARCH METHODOLOGY

Synthesis

Phosphorus is often synthesised via solid state reactions as the samples produced by these processes have excellent shape and luminescence. The solid-state reaction technique is used to create the $\text{Ba}_{2-x}\text{MgSi}_2\text{O}_7:x\text{Ce}^{3+}$ phosphors. BaCO_3 (99.0%), MgO (99.0%), $\text{SiO}_2 \cdot \text{H}_2\text{O}$ (99.0%), and rare earth oxide

CeO₂ (99.0%) were the initial reagents. Additionally, 0.05 mole of H₃BO₃ was utilised. After weighing the raw materials stoichiometrically and thoroughly mixing them for about two hours in an agate mortar, they were sintered for about four hours at 12000C. The formula for the reagent's reaction is $2.BaCO_3 + MgO + 2SiO_2 .H_2 O + CeO_2 = Ba_2MgSi_2O_7: Ce + 2H_2 O + 2CO_2 + O_2$

The Bruker D2 phaser X-ray powder diffractometer is used to identify the phase, and a Shimadzu UV-1700 UV-visible spectrometer was used to record absorption spectra in the 190–500 nm range. Thermoluminescence experiments were conducted using a TLD reader (Nucleonix TL 10091) and an 80W UV lamp as a 365 nm excitation source. An indigenous arrangement using an RCA 931 photomultiplier tube was used to monitor the ML. Interference filters were used to capture TL spectra.

Results and Discussions

XRD

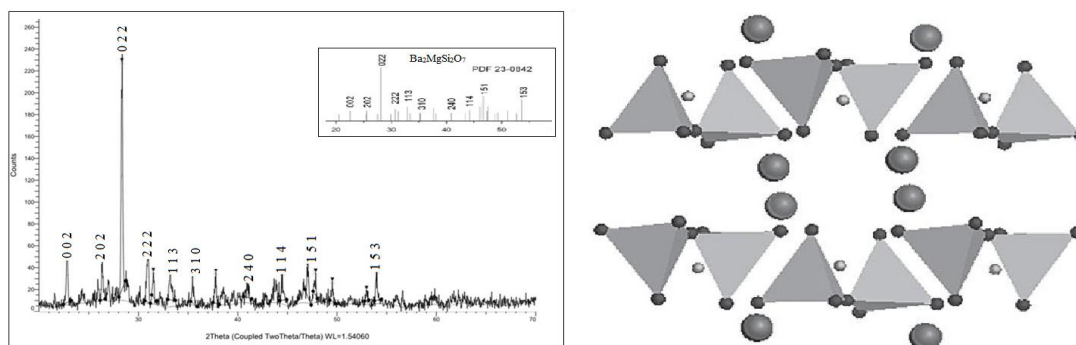


Fig.1 (a) XRD pattern of Ba_{1.95}MgSi₂O₇:0.05Ce³⁺ phosphor (b) Crystal Structure of Ba₂MgSi₂O₇

The XRD pattern was obtained between 20° and 2Θ and 70°. The host's lattice structure was not substantially altered by the doped Ce³⁺ ions. Using the Debye-Sherrer equation, the particle size for the (0 2 2) peak is 52.18 nm (Fig. 1(a)).

Table 1, Cell parameters, particle size and structure of the phosphor

Material	Cell parameters(nm)	Size (nm)	Structure
Ba _{1.95} MgSi ₂ O ₇ :0.05Ce	a = 0.8437, b=1.0727 c=0.8443	52.18	monoclinic

EDX Analysis

Energy-dispersive X-ray spectroscopy is an analytical method for determining a sample's elements. An energy-dispersive spectrometer can detect the quantity and energy of X-rays released by a specimen. The elemental composition of the specimen may be determined because the energy of the X-rays is indicative of the energy differential between the two shells and the atomic structure of the element from which they were released.

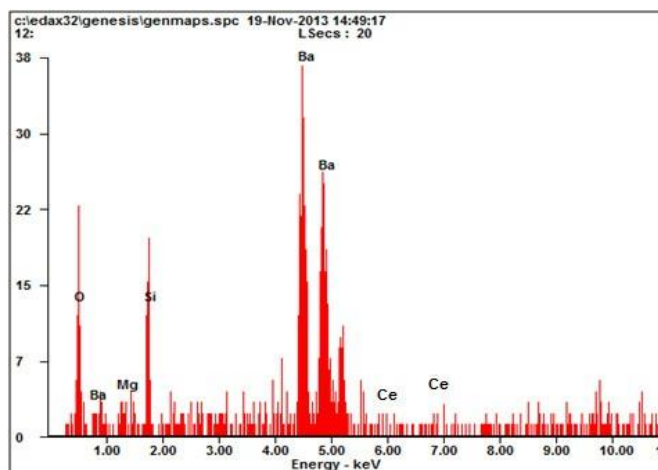


Fig.2 EDX analysis of Ba_{1.95}MgSi₂O₇:0.05Ce³⁺. Data was collected using Quanta 200F.

All of the essential elements are present in the sample, and no additional impurities are mixed, according to the EDX spectrum of Ba_{1.95}MgSi₂O₇:0.05Ce³⁺ (Fig. 2).

Table 2, Presence of expected elements in Ba_{1.95}MgSi₂O₇:0.05Ce³⁺ by weight% and atomic weight%

Element	Weight%	At%
O	17.16	48.00
Mg	06.36	11.70
Si	12.17	19.38
Ba	63.12	20.56
Ce	01.20	00.35

Photoluminescence Characteristics

The excitation and emission spectra of Ba_{1.95}MgSi₂O₇:0.05Ce³⁺ are shown in Fig. 3. The purplish-blue band emission peak at 415 nm and the excitation peak at 327 nm are shown by the phosphor and are caused by the 5d to 4f transition of the Ce³⁺ ion in Ba_{1.95}MgSi₂O₇:0.05Ce³⁺ phosphors.

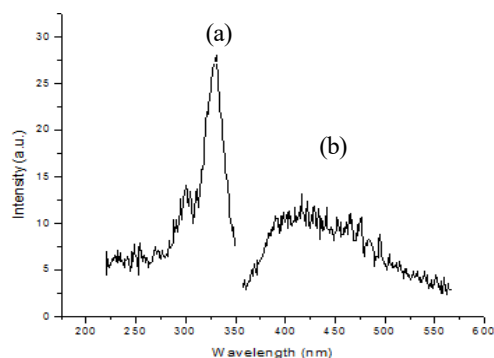


Fig.3 PL (a) Excitation and (b) Emission Spectra of Ba_{1.95}MgSi₂O₇:0.05Ce³⁺

Absorption Spectra

The term "absorption spectroscopy" describes spectroscopic methods that quantify how much radiation is absorbed as a function of wavelength or frequency as a result of contact with a material. A dramatic rise in absorption at the wavelength corresponding to the band gap energy results from the significant allowance of optical excitation of electrons across the band gap. The optical absorption edge is the name given to this characteristic of the optical spectrum. The absorption spectra of Ba_{1.95}MgSi₂O₇:0.05Ce³⁺ phosphors in the 190–500 nm range are shown in Fig. 4. It is evident that the spectrum is featureless and that there is no absorption at wavelengths longer than 390 nm (visible). The associated band gap is determined to be 4.96 eV, and the absorption edge is found to reside at 250 nm.

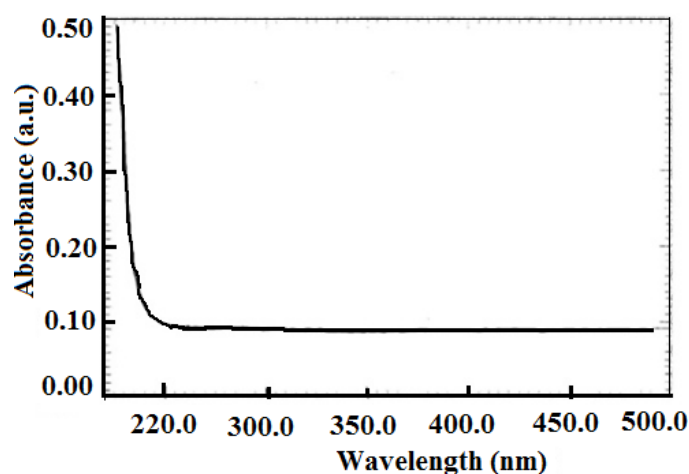
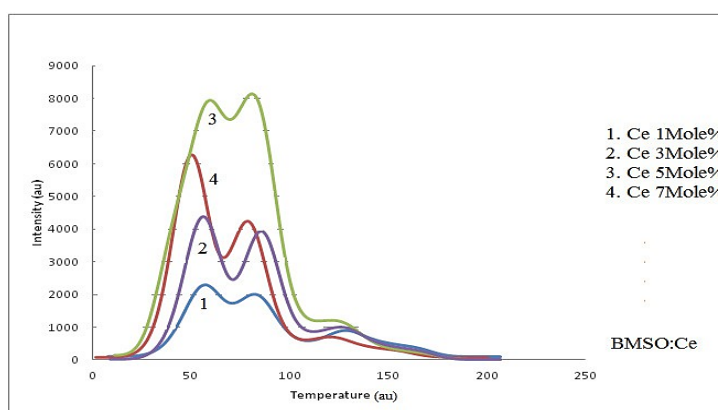


Fig.4 Absorption Spectra of Ba₂MgSi₂O₇:Ce

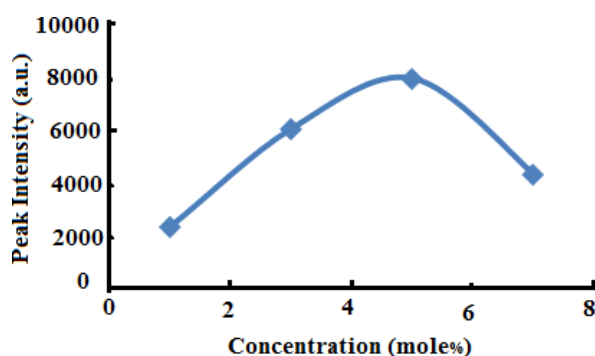
Thermoluminescence Characteristics

Ba₂MgSi₂O₇:Ce³⁺ Various dopants were used to synthesise phosphors. For TL, the doping concentration was ideal. The TL glow curve of Ba₂MgSi₂O₇:Ce³⁺ with varying Ce³⁺ concentrations

during 25 minutes of UV irradiation is shown in Fig. 5. The energy that the ions can store rises as the activator concentrations rise. Conversely, the energy transfer occurs when the distance between the activators decreases. As shown in Fig. 5(a) and (b), there is an activator concentration optimum as a result. The TL intensity reaches its maximum at Ce^{3+} values of 0.05 mole. The light curve between ambient temperature and 300°C shows two TL peaks. Using distinct heating rate methods, the trap depths for the two peaks were determined to be 0.08704 eV for the shallow trap and 0.4105 eV for the deep trap. The TL light curve for UV-irradiated $\text{Ba}_{1.95}\text{MgSi}_2\text{O}_7:0.05\text{Ce}^{3+}$ phosphors is shown in Fig. 6(a). From one minute to thirty minutes, the irradiation time was changed. It is evident that the TL intensity reaches its peak after 25 minutes of irradiation. The TL emission spectra of $\text{Ba}_2\text{MgSi}_2\text{O}_7:0.05\text{Ce}^{3+}$ phosphors are shown in Fig. 6(b). The 5d to 4f transition of Ce^{3+} is responsible for the greatest TL emission at 400 nm. Lattice flaws in phosphors are often the source of traps. The trapping concentration rises together with the initial UV irradiation period, which in turn causes the TL intensity to rise. The bleaching of trapped centres occurs after an optimal radiation period, and the TL intensity drops as the irradiation duration is increased further.



(a)



(b)

Fig. 5 (a) TL glow curve of Ce^{3+} doped $\text{Ba}_2\text{MgSi}_2\text{O}_7$ for different concentration of Ce^{3+} with 25

min UV radiation time. (b) Plot between Ce^{3+} concentration and total TL Intensity with UV dose for 25 min.

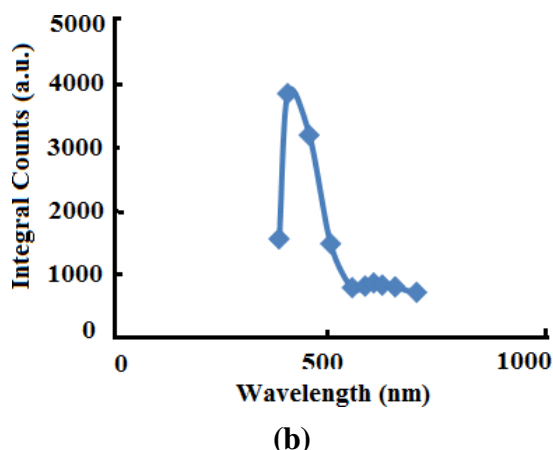
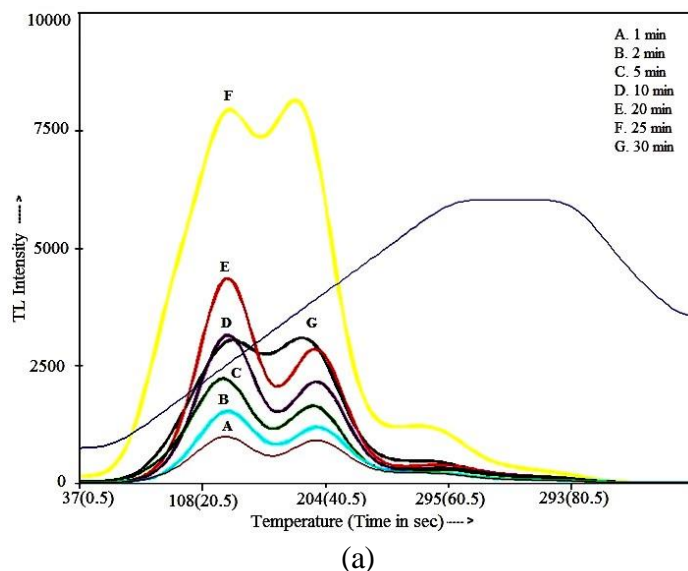
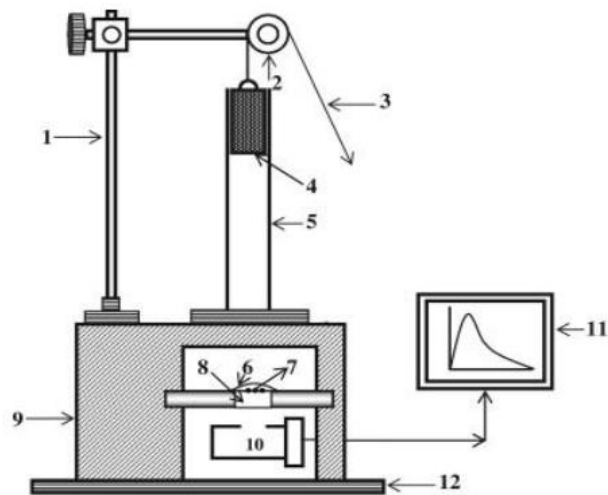


Fig. 6 (a) TL glow curve for $Ba_2MgSi_2O_7:0.05Ce^{3+}$ for different UV radiation time. (b) TL emission spectra of $Ba_{1.95}MgSi_2O_7:0.05Ce^{3+}$

Chemiluminescence Characteristics

A certain mass and shape load was dropped from varying heights to strike the phosphors at varying impact velocities in order to detect the chemiluminescence. Phosphorus was put on the Lucite plate and covered with thin aluminium foil for impulsive ML measurement. A storage oscilloscope attached to the PC was used to record the rise and fall of ML at various impact velocities. The experimental setup for the impulsive stimulation of ML is shown in Fig. 7 below.



1. Stand 2. Pulley 3. Metallic 4. Load 5. Guiding Cylinder 6. Aluminum foils 7. Sample 8. Transparent Lucite Plate 9. Wooden Blok 10. Photomultiplier tube 11. Digital storage oscilloscope 12. Iron base mounted on table

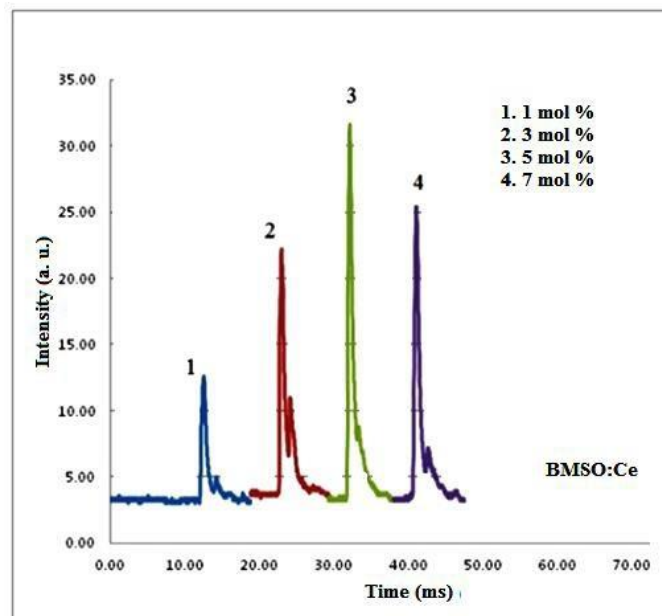
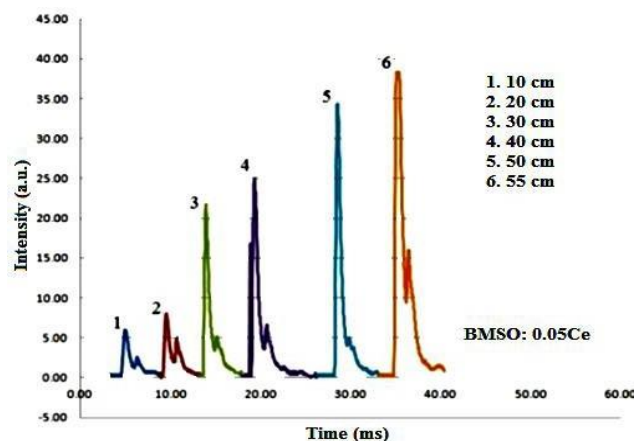


Fig.7 The experimental setup for the impulsive excitation of ML

(a)



(b)

Fig.8 (a) ML of Ba_{1.95}MgSi₂O₇:0.05Ce³⁺ for different concentration with 50 cm height. (b) ML intensity with different heights of Ba_{1.95}MgSi₂O₇:0.05Ce³⁺.

The greatest ML intensity was observed at a height of 50 cm and a Ce³⁺ concentration of 0.05 mole (Fig. 8(a)). Additionally, it was noted that the ML intensity rose linearly as the moving piston's lowering height increased (Fig. 8(b)). The movement of a crack creates charged surfaces as the ML phosphor fractures. The freshly formed oppositely charged surfaces may generate an electric field of magnitude 10⁷–10⁸ Vm⁻¹. The crystals may dielectrically break down in this field, and recombination luminescence may result from the recombination of free carriers. The concentration of the electron-hole pair formed during fracture rises in tandem with the doping concentration. Consequently, recombination luminescence rises as well. On the other hand, when the doping concentration rises, the distance between the free charge carriers grows closer, which causes energy transfer between them and lowers luminosity. The area of shattered charged surfaces grows with increasing impact height, which in turn causes an increase in recombination luminescence.

CONCLUSION

High-energy radiation dosimetry may benefit from the potential chemiluminescent characteristics of barium-containing phosphors. A well-defined TL glow curve, with high sensitivity, strong linearity in dose response, and minimum fading, is produced by their capacity to capture and release charge carriers upon radiation exposure. The study's findings support the notion that barium-based phosphors provide dependable dosimetric performance, especially when doped with appropriate rare-earth elements. These phosphors' high TL intensity is a major plus as it enables accurate radiation dose measurements across a broad spectrum. Medical radiation treatment, industrial radiation processing, and environmental radiation monitoring are just a few of the areas that may benefit from their linear response up to 10 Gy. Furthermore, the trapped charge carriers' stability—shown by their low signal fading over a 30-day period—improves their suitability for evaluating long-term radiation exposure.

Dosimetric uses of these materials are further supported by the activation energy estimates, which show deep and stable trap levels. Based on the results, it seems that barium-containing phosphors may be even more effectively chemiluminescent if dopant concentrations were optimised and other production

techniques were investigated. Research in the future should focus on creating new host matrices, refining methods for kinetic modelling, and finding more uses for these materials. Finally, radiation dosimetry benefits from the exceptional TL characteristics shown by barium-containing phosphors. Their promise as dependable dosimetric materials is highlighted by their excellent sensitivity, dose-response linearity, and long-term stability. They will become even more vital in precise and efficient radiation measurement as synthesis methods and materials are optimised to provide even better results.

REFERENCES

1. McKeever, S.W.S. (1985). *Thermoluminescence of Solids*. Cambridge University Press.
2. Chen, R., & McKeever, S.W.S. (1997). *Theory of Thermoluminescence and Related Phenomena*. World Scientific.
3. Bos, A.J.J. (2006). Theory of thermoluminescence. *Radiation Measurements*, 41(1), 45-56.
4. Yuhikara, E.G., & McKeever, S.W.S. (2011). *Optically Stimulated Luminescence: Fundamentals and Applications*. Wiley.
5. Cameron, J.R., & Zimmerman, D.W. (1961). Thermoluminescent dosimetry. *Health Physics*, 6(3), 188-191.
6. Tsujimura, T. (2017). *Phosphor Handbook*. CRC Press.
7. Viji, D.R. (2003). *Luminescence of Solids*. Springer.
8. Horowitz, Y.S. (1984). *Thermoluminescence and Thermoluminescent Dosimetry*. CRC Press.
9. Markey, B.G., McKeever, S.W.S., & Akselrod, M.S. (1995). Thermoluminescence of Al₂O₃:C. *Radiation Measurements*, 24(4), 457-463.
10. Chen, R. (2001). Glow curve analysis and its applications. *Nuclear Instruments and Methods in Physics Research Section B*, 184(1), 100-122.
11. Furetta, C. (2010). *Handbook of Thermoluminescence*. World Scientific.
12. McKeever, S.W.S. et al. (1996). Advances in Thermoluminescence Dosimetry. *Radiation Protection Dosimetry*, 66(1-4), 295-302.
13. Bos, A.J.J., & Pijters, T.M. (2000). Thermoluminescence kinetics of dosimetric materials. *Radiation Protection Dosimetry*, 88(1), 1-9.
14. Bøtter-Jensen, L. et al. (2003). Luminescence Dosimetry. *Radiation Measurements*, 37(4-5), 535-541.
15. Pagonis, V. et al. (2007). *Numerical and Practical Exercises in Thermoluminescence*. Springer.

16. Chen, R., & Lawless, J.L. (1998). Anomalous TL properties of phosphor materials. *Journal of Luminescence*, 76-77, 184-193.
17. Kalita, J.M. et al. (2012). TL response of rare-earth doped phosphors. *Journal of Applied Physics*, 111(8), 084504.
18. Vij, D.R., & Singh, N. (2009). *Optical and Luminescence Properties of Doped Materials*. Nova Science Publishers.
19. Moscovitch, M. et al. (2000). Advances in TLD materials and techniques. *Radiation Protection Dosimetry*, 89(1-2), 109-118.
20. Bøtter-Jensen, L., Bulur, E., Duller, G.A.T., & Murray, A.S. (2000). Thermoluminescence and optically stimulated luminescence. *Radiation Measurements*, 32(5-6), 523-528.